Available online at www.sciencedirect.com
SCIENCE DIRECT®
Journal of Catalysis 219 (2003) 295–304
JOURNAL OF CATALYSIS
www.elsevier.com/locate/jcat

Catalytic studies on ceria lanthana solid solutions II. Oxidation of carbon monoxide

M.F. Wilkes, P. Hayden, and A.K. Bhattacharya *

Warwick Process Technology Group, Department of Engineering, University of Warwick, Coventry CV4 7AL, UK

Received 9 January 2003; accepted 27 January 2003

Abstract

The catalytic combustion of carbon monoxide over ceria, lanthana, and their mixed oxides has been studied under reaction conditions free from heat and mass transfer limitations. The bulk structures, surface compositions, and surface areas of the catalysts were determined by XRD, XPS, and BET methods, respectively. Doping either ceria or lanthana with low levels of the other oxide retards the reaction. The reaction order on carbon monoxide is almost first-order over ceria, but over the lanthana-containing catalysts it changes from positive to negative with increasing partial pressure. With all catalysts, the rate tends to zeroth order on oxygen with increasing partial pressure. An extended study was made of the major solid solution, lanthana-in-ceria, which operated near-threshold temperatures is poisoned by lanthana. The active centres are ensembles of cerium atoms, the size being lowered by lanthanum. The retardation is discussed in terms of interactions between cerium ensembles and anionic vacancies.

Keywords: Carbon monoxide; Combustion; Carbon dioxide; Ceria; Lanthana; Mixed oxide; Poisoning

1. Introduction

The catalytic activity of ceria in the oxidation of carbon monoxide is well known. Rienaker and co-workers reported the efficacy of pure ceria and of its mixed oxides with alumina [1], thoria [2], and lanthana [3]. Catalytic activity was associated with electrical conductivity and lattice structure, although these early authors recognised that to enable accurate formulation of the reaction mechanism a quantitative analysis of the catalyst surface was required. In the case of pure ceria, the transfer of lattice oxygen to adsorbed carbon monoxide was confirmed as an oxidation route in several laboratories [4–8]. Breysse et al. [4,5] further related the catalyst activity of pure ceria directly to its electrical conductivity when the latter alters in response to the concentration of intrinsic anionic vacancies, these in turn being controlled by reactant partial pressures. Theoretical treatments have rationalised the mechanism of oxygen transfer [9–11], supposing that intrinsic oxygen vacancies play a pivotal role in the catalytic oxidation of carbon monoxide. Modelling the oxidation of carbon monoxide by oxygen transfer from ceria has been predicted to be exothermic at the surface, especially at the (110) and (310) surfaces, but endothermic in the bulk [9]. However, this stems mainly from the dependence of the substitution energy of Ce^{4+} for Ce^{3+} in the lattice rather than the contribution to the reaction enthalpy from the energy of the formation of the vacancy.

In a review of the catalytic oxidation of carbon monoxide by ceria-based materials, Trovarelli [12] proposed two mechanisms: a stepwise redox mechanism and a concerted mechanism. In the former, adsorbed carbon monoxide is oxidised by transfer of lattice oxide that is replenished by adsorption of molecular oxygen on the transient oxygen vacancy. In the concerted mechanism adsorbed carbon monoxide reacts with an active surface oxygen.

Doping ceria with lower valent cations creates oxygen vacancies, manifested by increased electrical conductivity [13]. Small such cations preferentially migrate to the surface [14], with the anion vacancies being expected to do likewise [11]. It has been proposed that the defective surface of these materials may enhance the catalytic properties of these doped solids relative to pure ceria [14]. Although several examples of cation segregation in oxide systems are known [15], it is perhaps surprising that doping ceria with a series of trivalent oxides had little or no effect on its cat-

* Corresponding author.
E-mail address: akb@warwick.ac.uk (A.K. Bhattacharya).

0021-9517/$ – see front matter © 2003 Published by Elsevier Inc.
doi:10.1016/S0021-9517(03)00045-9

alytic activity for the oxidation of carbon monoxide: activity did not correlate with either the concentration of extrinsic anion vacancies or oxygen mobility [16]. In fact, Rienaker and Wu [3] reported that doping ceria catalysts with lanthana retarded the oxidation despite later being effective in stabilising the catalysts' surface areas, a feature attributed to an association of an oxygen vacancy with its progenitor dopant ion [17]. Thus, superficially extrinsic oxygen vacancies appear not to promote the catalytic oxidation of carbon monoxide.

A possible determinant of catalytic activity, claimed for the promotion of methane combustion by partial substitution of Ce in ceria with isovalent ions, is crystallite size where the smaller, more defective fluorite structures are credited with raising activity *via* increased oxygen mobility [18]. However, we would respectfully point out that, indexed relative to their surface areas, this range of catalysts exhibited no increase in their specific activities.

Kundakovic and Flytzani-Stephanopoulos [19] alternatively attributed the promotion by lanthana of the ceria-catalysed oxidation of methane to several factors, including smaller ceria crystal size, increased reducibility, and the introduction of extrinsic oxygen vacancies.

Despite catalysis being a surface phenomenon, none of the past studies of catalytic activity correlated catalyst performance with the composition of the surface.

To explore the source of the activation in the catalytic oxidation of carbon monoxide, the aim of the present work was to measure the specific activities, crystallite sizes, and surface compositions, identify the bulk structures, and sketch reaction kinetics over the entire composition range of ceria–lanthana mixed oxides. Over the major part of the compositional range, up to $x = 0.6$ in $Ce_{1-x}La_xO_{2-x/2}$, the general formula for these mixed oxides, lanthana forms a solid solution in ceria; above $x = 0.9$, ceria forms a solid solution in lanthana; the range between $x = 0.6$ and $x = 0.9$ results in the formation of mixed phases [20]. Although activity indices over the whole range of oxide compositions are presented here, the complexity of the responses outside the lanthan-in-ceria solutions enforces a postponement of their detailed analysis. At this stage, we have focused on the behaviour of the latter solutions. A minor study of dopants other than lanthana is included.

2. Experimental

2.1. Catalyst preparation

Mixed oxide catalysts of the general formula $Ce_{1-x}La_xO_{2-x/2}$ were prepared by co-precipitation from nitrates ($Ce(NO_3)_3 \cdot 6H_2O$ (99.99%, Alfa), $La(NO_3)_3 \cdot 6H_2O$ (99.999%, Aldrich)) with ammonium bicarbonate, washed free of alkali, dried in air at 110 °C, powdered, decomposed in air at 450 °C, calcined at 800 °C for 8 h and sized to 200–400 μm. Before catalytic reaction testing, the stored samples were heated to 600 °C in air.

2.2. Reactor

Gases of known composition are introduced from cylinders via Brooks 5850 mass flow controllers. The microreactor consists of $\frac{1}{4}$-, $\frac{1}{8}$-, and $\frac{1}{16}$-in. stainless steel tubs connected using Swageloc fittings. The system is operated at atmospheric pressure, with negligible pressure drop across the catalyst bed. The reactant gases were mixed in the manifold section, which included a 7-μm filter, pre-heated to 120 °C, and delivered to a heated quartz reaction tube. The fixed catalyst bed consists of a cylindrical plug of 200- to 400-μm catalyst particles, 10-mm length, and 4-mm diameter. Product gases were analysed by gas chromatography (Hewlett-Packard model 5890) using a Carboxen 1000 column and mass spectroscopy (Fisons Instruments).

2.3. Catalyst testing

The catalyst bed comprised a weighed amount (about 0.2 g) of particles (200–400 μm) located within a quartz tubular reactor (4-mm i.d.) packed, with tapping, into a length of at least 20 mm. The reacting gases were delivered as 10% CO in nitrogen (25 ml/min) and 21% O_2 in helium (118 ml/min), generating a linear gas velocity of 19 cm/s. At 380 °C, tests showed that the oxidation rate increased with linear gas velocity up to about 10 cm/s and thereafter remained invariant with a gas rate up to 40 cm/s. The conversion of carbon monoxide and the formation of carbon dioxide were measured: the mass balance was $100 \pm 3\%$ with 95% confidence limits.

2.4. Temperature-programmed desorption (TPD)

Following initial TPDs in a helium carrier and subsequent adsorption of carbon monoxide at 340 °C for 1 h, two classes of TPD were performed: oxidative single-stage and two-stage TPD, first in a helium carrier and then in oxygen-in-helium.

3. Results

3.1. Oxidation rate as a function of mixed oxide composition: effect of x in of $Ce_{1-x}La_xO_{2-x/2}$

The stationary reaction rate at 310 °C formed the basis of this comparative study of catalyst activity as a function of oxide composition. Pass-conversions of carbon monoxide were in the range 0.3–5%. The results are presented in Fig. 1 as functions of bulk and surface compositions.

Doping either ceria or lanthana with low levels of the other oxide strongly retards catalyst activity. Up to the lanthana-in-ceria solution limit in the range bulk $x = x_b =$

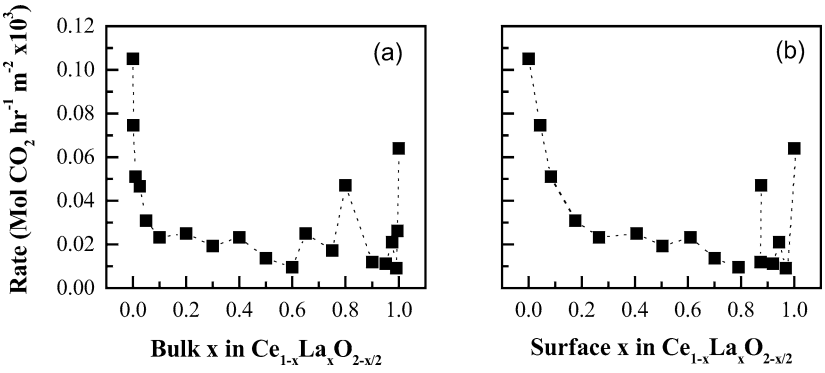

Fig. 1. Specific activity as a function of mixed oxide composition: (a) bulk and (b) surface.

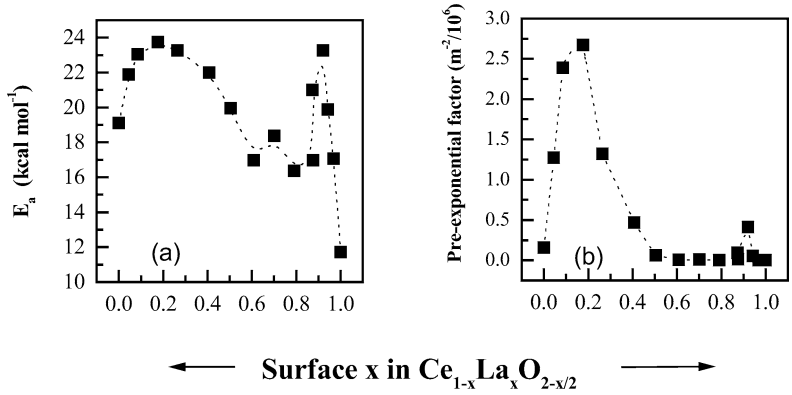

Fig. 2. Apparent energy of activation (a) and apparent specific pre-exponential factor (b) as functions of the catalyst surface composition.

0.5–0.6 [20], the catalytic activity diminishes progressively with addition of lanthana. Above this limit, in exhibiting two maxima, the patterns of activity become extremely irregular.

Analyses of the surface segregation isotherms of the lanthana-in-ceria solutions result in simple empirical representations, suggesting consistency of their surface structures and energies [20]. Since catalysis is a surface phenomenon, this encourages the presentation of the results in terms of the surface composition.

The temperature dependencies of the activities enable their resolution into apparent energies of activation and apparent specific pre-exponential factors. These are displayed as functions of the surface composition in Fig. 2.

The dependence of the apparent energy of activation on the composition of the surface of this range of mixed oxides is complex. It may be viewed as exhibiting two maxima: a rounded first peak achieved at between a surface lanthanum ionic fraction, x_S, of 0.1 and 0.2, and a second sharp peak at x_S of 0.9.

Similar to the composition dependency of the energy term, the pre-exponential factor shows two maxima: a high first peak at between x_S of 0.1 and 0.2 and a second low peak at x_S of 0.9. Strong compensation effects are apparent: with lanthana-in-ceria solutions, the progressively decreasing catalytic activity induced by lanthana is resolved into single peaks in both the activation energy and pre-exponential terms whereas with ceria-in-lanthana solutions, the two activity maxima are replaced by single peaks when the surface lanthanum ionic fraction is about 0.9. The pair of theta equations is, respectively,

$$\ln(\mathrm{A}) = -6.5 + 1.0E,$$

$$\ln(\mathrm{A}) = -1.5 + 0.7E.$$

With the lanthana-in-ceria solid solutions, our main theme, the concentration-dependent retardation of catalytic activity is attributed to an increasing energy of activation at low levels of lanthanum and to a decreasing pre-exponential factor at high levels.

To summarise, with the lanthana-in-ceria solutions, increasing levels of lanthana progressively retard the catalytic action of ceria yet exhibit a maximum in the energy of activation and the pre-exponential factor. We have already established that these solutions exhibit surface segregation isotherms with consistent descriptive constants. With the ceria-in-lanthana solutions, the patterns of activity are irregular in exhibiting two maxima, although these reduce to a single maximum in the energy of activation and pre-exponential factor responses. At this stage, our study of the segregation isotherms and other data describing the latter solutions is incomplete, and consequently, beyond an outline description of the pure lanthana case, we shall concern ourselves only with the catalytic action of lanthanides in ceria.

Table 1
Oxidation rate as a function of composition of $Ce_{1-x}Ln_xO_{2-x/2}$

Ce $(1-x)$	La	Pr	Gd	Nb	Surface area (m^2/g)	Rate (mol of CO_2/(h kg)) (310 °C)	Specific rate (mol of CO_2/(h m^2)) ($\times 10^3$) (560 °C)
1	0	0	0	0	15.2	1.593	0.105
0.8	0.2	0	0	0	13.9	0.347	0.025
0.8	0	0.2	0	0	17.9	0.559	0.031
0.8	0.1	0.1	0	0	19.0	0.561	0.029
0.8	0	0	0.2	0	18.6	0.350	0.019
0.975	0.025	0	0	0	12.93	0.603	0.047
0.98	0	0	0	0.025	15.0	1.53	0.104

3.2. Oxidation rate as a function of mixed oxide composition: effect of Ln in of $Ce_{1-x}Ln_xO_{2-x/2}$

Table 1 presents the variation in oxidation rate with mixed oxides of ceria with lanthana, gadolinia, preseodymia, and niobia.

Gadolinia and preseodymia retard the catalytic activity of ceria to a degree similar to that exhibited by lanthana, whereas niobia has no effect.

3.3. Kinetics of catalytic oxidation

3.3.1. Over ceria

The responses to changing the partial pressures of carbon monoxide, oxygen, and carbon dioxide, at constant partial pressures of the other two gases, are presented in Fig. 3.

The apparent order on CO partial pressure is approximately 0.8, which is in good agreement with that reported by Breysse [21]. Alternatively and preferably the results may be represented by the Langmuir-type isotherm expression:

$$\text{rate} = 1.3(\%\text{CO})\big/\big(1 + 0.3(\%\text{CO})\big). \tag{1}$$

Adsorption of CO on ceria has been reported as obeying a Langmuir adsorption isotherm [22]. At the partial pressures generated by the product carbon dioxide, its retardation effect is negligible (see later).

The responses of the rate of oxidation to changes in oxygen partial pressure are dependent on the duration of the test. When the oxygen partial pressure is raised, the initial rate diminishes with time. When the oxygen partial pressure is lowered, the reverse phenomenon is observed. The results presented here are the stationary rates achieved after an extended period of operation. At low oxygen partial pressures, the rate of the CO oxidation reaction is found to increase in proportion to the square root of oxygen partial pressure, P_{O_2}. Further increases in P_{O_2} have progressively less effect on the reaction rate, eventually establishing an apparent zeroeth order. The effect of the full range of P_{O_2} can be represented by the expression

$$\text{rate} = 27\sqrt{(\%\text{O}_2)}\big/\big(1 + 9\sqrt{(\%\text{O}_2)}\big). \tag{2}$$

The retardation of the oxidation by carbon dioxide was measured by its inclusion in the reaction feed gases. The response may be represented by the equation

$$\text{rate} = \frac{1.8}{[1 + 0.1(\%\text{CO}_2) + 0.01(\%\text{CO}_2)^2]}. \tag{3}$$

3.3.2. Over lanthana

The responses to changing the partial pressures of carbon monoxide, oxygen, and carbon dioxide, at constant partial pressures of the other two gases, are presented in Fig. 4.

At the threshold temperature of 310 °C, the catalytic oxidation rate increases faster than first order with CO pressure but the low pass yields limit the accuracy of the data. Operating at higher temperatures improves the quality of the data, which is modelled later. At 340 and 370 °C, Fig. 4a shows

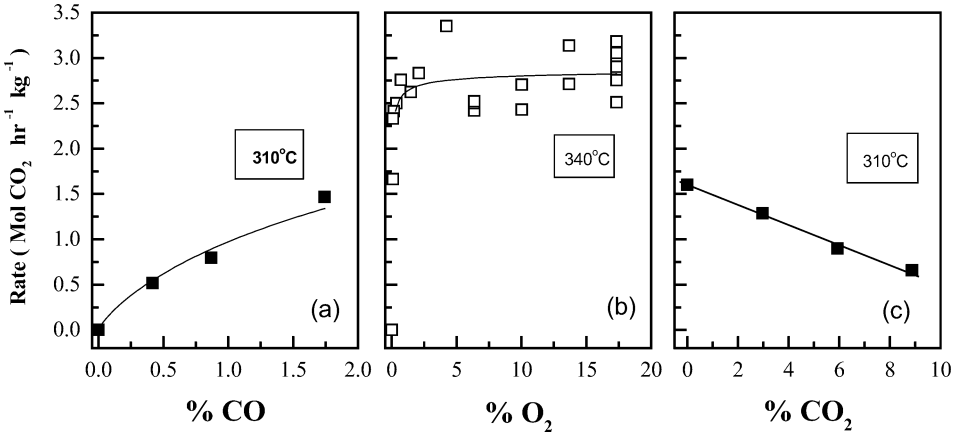

Fig. 3. The responses of the reaction rate over ceria to the partial pressures of (a) carbon monoxide, (b) oxygen, and (c) carbon dioxide.

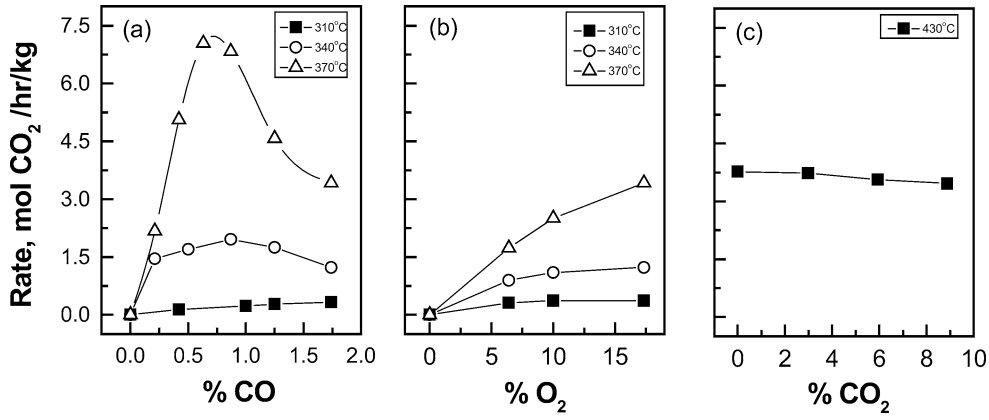

Fig. 4. The responses of the reaction rate over lanthana to the partial pressures of (a) carbon monoxide, (b) oxygen, and (c) carbon dioxide. The solid lines at the highest temperatures correspond to the model.

the positive responses at low CO pressures becoming negative at high CO pressures.

In contrast to the hysteresis exhibited with ceria catalysts, stationary rates of oxidation were quickly established after step changes in oxygen partial pressure. The data in Fig. 4b show the reaction order on P_{O_2} ranging from 0.3 to 0.7 at 340 and 370 °C, respectively, generating a mean value of 0.5. Compared to the strong retardation by carbon dioxide over ceria, Fig. 4c shows its effect on carbon monoxide oxidation over lanthana to be weak.

Carbon dioxide is adsorbed on lanthana with a range of binding strengths yet the apparent activation energy (not shown) of the oxidation of carbon monoxide was changed little by the presence of carbon dioxide. It may be concluded that the carbon dioxide is only weakly adsorbed on the sites active in the catalytic oxidation of carbon monoxide over lanthana.

3.3.3. Over $Ce_{0.95}La_{0.05}O_{1.875}$

The responses of the reaction to changing the partial pressures of carbon monoxide, oxygen, and carbon dioxide over this oxide are presented in Fig. 5, where they are also compared to models developed later.

3.4. Temperature-programmed desorption

The results of the single-stage oxidative desorptions are presented in Fig. 6. Up to a surface lanthanum ionic fraction of 0.79, corresponding to the bulk solubility limit of lanthana-in-ceria, the amount of absorbed carbon monoxide increases smoothly in approximate proportion to the lanthanum content. Above this level, the adsorption pattern changes to include a maximum. Table 2 presents the results of the two-stage TPDs. Adsorption of carbon monoxide on ceria as carbonyl, carbonite (CO_2^{2-}), and carbonate, the latter with concomitant reduction of ceria [12,22], is manifested by the major release as carbon dioxide in the first-stage desorption. Despite its much lower surface area, lanthana adsorbs far more carbon monoxide, releasing some as carbon dioxide in the first-stage desorption but additionally generating a carbonaceous residue desorbed as carbon dioxide in the oxidative second-stage desorption.

3.5. Crystal size of $Ce_{1-x}La_xO_{2-x/2}$ catalysts

It has been suggested that crystallite size is a determinant of the catalytic activity of ceria systems in the oxidation of

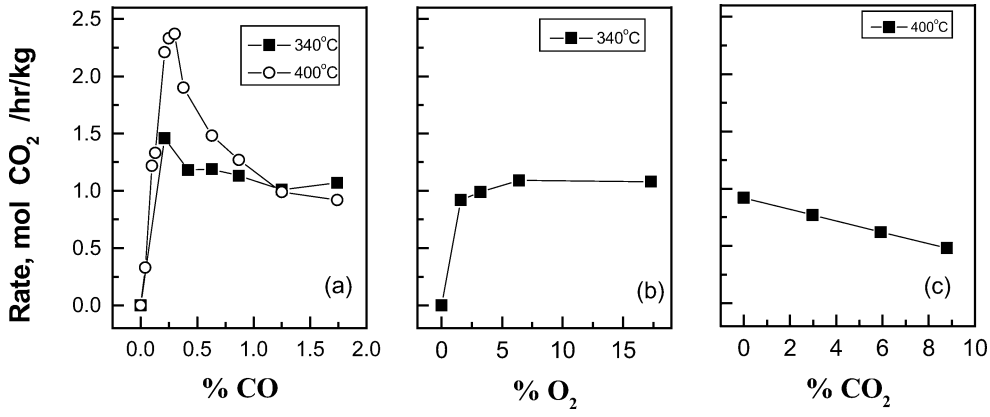

Fig. 5. The responses of the reaction rate over $Ce_{0.95}La_{0.05}O_{1.875}$ to the partial pressures of (a) carbon monoxide, (b) oxygen, and (c) carbon dioxide.

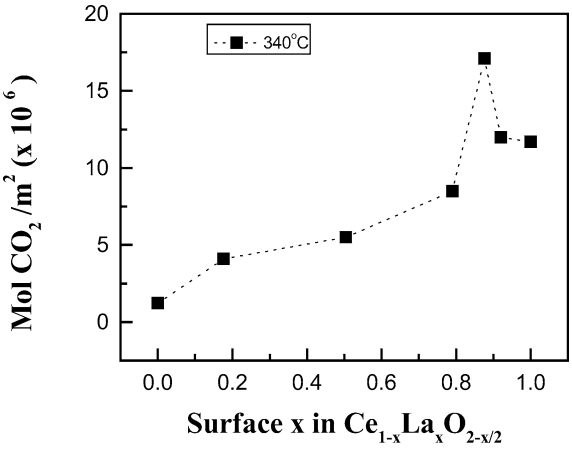

Fig. 6. The specific oxidative desorption of carbon monoxide adsorbate (formed at 340 °C) as a function of mixed oxide surface composition.

Table 2
The desorption of carbon oxides following adsorption of carbon monoxide on ceria and lanthana (desorbate as µmol per square metre of oxide)

Oxide	1st TPD		2nd TPD	
	CO	CO_2	CO	CO_2
Ceria	1.6	1.4	0	0.2
Lanthana	8.7	4.6	0	1.8

methane [19]. To test this hypothesis in the present case, data on the crystal size and specific activity of the present range of pure and mixed oxide catalysts are displayed in Fig. 7. Fig. 7a shows that increasing the lanthanum atomic fraction results in progressively smaller crystal sizes and decreasing specific activities until a minimum is reached in the range $x = 0.6$–0.7, the solubility limit of lanthana in ceria, after which additional lanthanum results in enlarged crystallites and higher specific activities. Stabilising crystallite size in lanthanum-doped ceria has been reported previously [17]. Fig. 7b visualises specific activity increasing with crystallite size.

4. Discussion

XRD of the present catalysts distinguished three structures formed over the complete range of oxide compositions: a solid solution of lanthana in ceria is formed up to a bulk lanthanum ionic fraction, x_b, of about 0.6; a mixed phase between x_b of 0.6 and 0.9; and a solid solution of ceria in lanthana when x_b exceeds 0.90. We have presented data on the physical characteristics of these catalysts and quantitatively modelled the surface segregation data elsewhere [20]. We aim to apply this data in the analysis of the present lanthanum concentration-dependent retardation of the ceria-catalysed oxidation of carbon monoxide. We have already noted that, over the range of the lanthana-in-ceria solution, the retardation increases smoothly with lanthanum concentration but that the patterns of activity become irregular at higher concentrations. For these reasons we confine the discussion to catalysts forming lanthana-in-ceria solutions.

The results also show that the apparent energy of activation and the pre-exponential factor respond systematically with surface-segregated lanthanum concentration, x_s, rising with x_s at low levels and falling at high levels.

A further refinement of the discussion is perhaps apt. The standard measurements of catalytic activity were performed at low partial pressures and close to the threshold reaction temperature of the least active catalysts using gas compositions with a twenty-fold stoichiometric excess of oxygen. At the conditions, the oxidation rate was almost zeroeth order in oxygen but responded to oxygen pressure if that were lowered by an order of magnitude. It always responded to carbon monoxide pressure; hence, it can be anticipated that the reactivity patterns will reflect the activation of carbon monoxide rather than of oxygen.

4.1. Kinetics over ceria

Over ceria, the reaction order is first, or nearly first, on carbon monoxide pressure, while the order on oxygen is more complex; it varies from half-order at low oxygen pressures to zeroeth order for higher pressures. Ceria exhibits

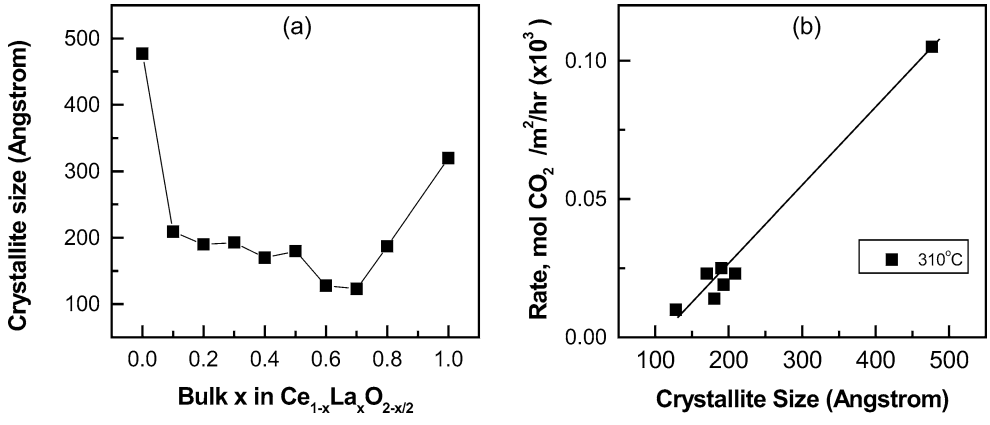

Fig. 7. (a) Crystallite size as a function of composition and (b) specific activity as a function of crystallite size.

partial reversible adsorption of carbon monoxide. A concerted reaction scheme is proposed that assumes Langmuir-style adsorption isotherms, a random distribution of sites, and an oxidation rate proportional to the product of the coverages of adsorbed carbon monoxide and adsorbed atomic oxygen:

$$O_{2(g)} + 2Ce^{3+} \leftrightarrow 2Ce^{3+}\text{–}O_{(ads)},$$
$$CO_{(g)} + Ce^{4+} \leftrightarrow Ce^{4+}\text{–}CO_{(ads)},$$
$$Ce^{3+}\text{–}O_{(ads)} + Ce^{4+}\text{–}CO_{(ads)} \rightarrow Ce^{3+} + Ce^{4+}\text{–}CO_{2(ads)},$$
$$Ce^{4+}\text{–}CO_{2(ads)} \leftrightarrow Ce^{4+} + CO_{2(g)},$$
$$Ce^{3+}\text{–}CO_{2(ads)} \leftrightarrow Ce^{3+} + CO_{2(g)},$$
$$\text{rate} = k(K_{O_2}P_{O_2})^{0.5}K_{CO}P_{CO} \Big/ \Big(\big(1 + (K_{O_2}P_{O_2})^{0.5} + K_{CO_2}^{Ce^{3+}}P_{CO_2}\big) \times \big(1 + K_{CO}P_{CO} + K_{CO_2}^{Ce^{4+}}P_{CO_2}\big)\Big). \quad (4)$$

At constant partial pressures of two of the three gases involved, this relationship reduces to reasonable descriptions of each of the three experimental responses of the oxidation rate over ceria to variations in the partial pressure of the third gas as shown in Fig. 3.

4.2. Kinetics over lanthana

Over lanthana, the response of the oxidation rate to partial pressure of carbon monoxide is complex: a second-order dependency at low partial pressures and a strong retardation at high partial pressures. Lanthana also exhibits partly reversible adsorption of carbon monoxide. A concerted oxidation process is proposed, comprising the following steps:

$$O_{2(g)} + 2S \leftrightarrow 2S\text{–}O,$$
$$nCO_{(g)} + S \leftrightarrow (CO)_n\text{–}S,$$
$$(CO)_n\text{–}S + S\text{–}O + S \rightarrow S\text{–}CO_2\text{–}S + (CO)_{n-1}\text{–}S,$$
$$(CO)_{n-1}\text{–}S + CO_{(g)} \leftrightarrow (CO)_n\text{–}S,$$
$$S\text{–}CO_2\text{–}S \leftrightarrow CO_{2(g)} + 2S.$$

S represents a site capable of adsorbing molecular oxygen dissociatively and of adsorbing CO in states such that n is greater than or equal to 2 (see later discussion of TPD results). The rate-limiting reaction is between the adsorbed carbon monoxide and adsorbed oxygen, provided there is an adjacent S site to adsorb the resulting carbon dioxide. On this basis,

$$\text{rate} = k_4 P_{CO}^n P_{O_2}^{1/2} \Big/ \big(1 + K_{CO}P_{CO} + K_{(CO)_2}P_{CO}^2 + \cdots + K_{(CO)_n}P_{CO}^n + K_1 P_{O_2}^{1/2} + K_{CO_2}P_{CO_2}\big)^2. \quad (5)$$

At constant partial pressures of oxygen and carbon dioxide Eq. (5) reduces to

$$\text{rate} = \frac{k_5 P_{CO}^n}{(1 + K_6 P_{CO} + K_7 P_{CO}^2 + \cdots + K_n P_{CO}^n)^2}. \quad (6)$$

Computerised curve fitting of the experimental data to Eq. (6) generates insignificant values for the terms containing K_6 and K_n compared to that based on K_7. With the simplified denominator, the fit is optimised at $n = 2$, enabling Eq. (6) to be written as

$$\text{rate} = \frac{k_2 P_{CO}^2}{(1 + K_{(CO)_2}P_{CO}^2)^2}, \quad (7)$$

where $k_2 = 56$ and $K_{(CO)_2} = 2$. Fig. 4a compares the experimental and modelled data at 370 °C.

At constant partial pressures of two of the three gases involved, Eq. (5) also reduces to reasonable descriptions of the responses to variations in the partial pressure oxygen and carbon dioxide as shown in Fig. 4.

4.3. Kinetics over the mixed oxide $Ce_{0.95}La_{0.05}O_{1.875}$

As over lanthana, the response of the oxidation rate to variation of the partial pressure of carbon monoxide is complex. The model, Eq. (8), is based on contributions from ceria-style and lanthana-style kinetics as expressed in Eqs. (4) and (7), respectively,

$$\text{rate} = \frac{a(\%CO)^2}{(1 + b(\%CO)^2)^2} + \frac{c(\%CO)}{1 + d(\%CO)}, \quad (8)$$

where a, b, c, and d are constants taking, at 400 °C, the values 121, 16, 3, and 3.4, respectively. Fig. 8 compares the experimental and modelled data. According to this model, some 85% of the oxidation rate would originate from the ceria-style component of Eq. (8). This compares with a surface atomic fraction of 0.82 cerium. The oxygen dependency may be represented by

$$\text{rate} = 3\sqrt{(\%O_2)} \Big/ \big(1 + 2.4\sqrt{(\%O_2)}\big). \quad (9)$$

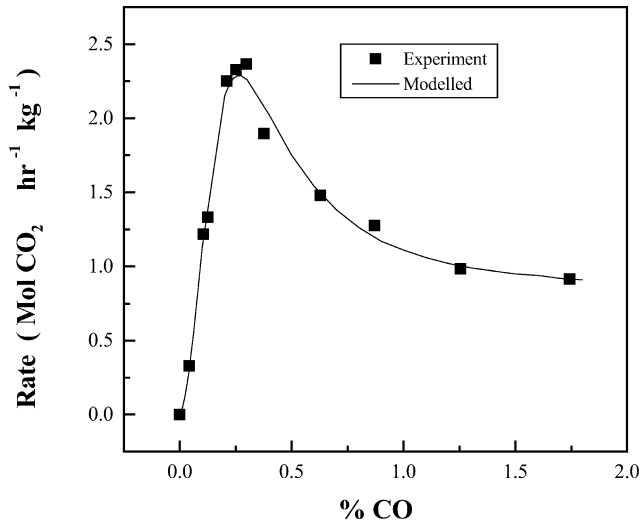

Fig. 8. Reaction rate as a function of carbon monoxide partial pressure over $Ce_{0.95}La_{0.05}O_{1.875}$.

4.4. TPD of carbon monoxide adsorbate

Both the ceria and lanthana catalysts studied here exhibited partially reversible adsorption of carbon monoxide in a helium atmosphere with the desorbate additionally containing carbon dioxide. The concomitant reduction of ceria affords a ready rationalisation of that source of carbon dioxide, where carbon monoxide adsorbate has been reported as containing linearly adsorbed CO, carbonates, and carbonites [12,22]. Carbon monoxide adsorbate on lanthana has been reported as comprising carbonite and ketenic dimer [23], but in contrast to the cerium case, the adsorbate contained a fraction, which was desorbed only after oxidation with molecular oxygen. It is likely that some scission of carbon–oxygen bonds occurred, possibly in a Boudouard-style disproportionation of adsorbed carbon monoxide. The essential point is that the carbon monoxide adsorbates on ceria and lanthana behaved very differently, providing the basis for a progressive change in the mechanism of the oxidation process across the composition range of the mixed oxides.

4.5. Effect of composition on catalyst specific activity

It is proposed that the activity of this range of catalysts stems from adsorbed atoms of oxygen interacting with adsorbed carbon monoxide, the latter existing as a monomer on ceria and as a dimer on lanthana. At the oxygen partial pressures used in the standard tests, the rate was essentially zeroeth order in oxygen. It is proposed that the changes in the specific reaction rate manifest variations in the activation of adsorbed carbon monoxide.

Over the composition range of the lanthana-in-ceria solid solutions, Fig. 1 shows the initial strong poisoning effect of lanthana progressively diminishes up to a surface atomic fraction of 0.8. Fig. 9a illustrates a modelled specific activity, which varies with the reciprocal of the exponential of the surface concentration of lanthanum, indicating a consistent poisoning coefficient of lanthanum. Alternatively, the data may be very approximately represented by the equation

$$\text{specific activity}_x = \text{specific activity}_0 \times (1 - x_s)^n, \qquad (10)$$

where specific activity$_x$ = specific activity at coverage x_s, specific activity$_0$ = specific activity over pure ceria, x_s = surface coverage by passivating lanthanum atoms, and n = number of cerium atoms in the active ensemble—a general relationship promulgated by Andersen et al. [24] to determine the critical size of active ensembles. The mean value of n is about 6, suggesting that the active site contains this number of cerium atoms. The fit is improved if n is evaluated as a function of x_s. Fig. 9b compares the experimental data and the Andersen model modified according to

$$n = 9.26 - 21.7x_s + 15.4x_s^2. \qquad (11)$$

From an initial value of about 9 in ceria, the apparent size of the active ensemble decreases linearly with x_s up to about $x_s = 0.1$–0.2 but thereafter increases as the second-order effect contributes more. However, such an analysis implies a common kinetic scheme across the range of compositions. Since this is not a characteristic of the present system, this interpretation of the poisoning requires some modification.

Zamar et al. [18] have discussed the effect of lanthana on the activity of the ceria-catalysed oxidation of methane in terms of a negative response to crystallite size. Contrastingly, Fig. 7b shows that, over the range of the fluorite-structured lanthana-in-ceria solid solutions, the specific activity increases almost linearly with crystallite size. Consequently, the Zamar argument is not applicable here. Instead, we interpret the effect of oxide composition in terms of a progressive shift from a cerium-style catalysis to one dominated by lanthanum. We shall propose that the retarding effect of lanthanum is induced by the clustering of oxygen vacancies rather than by the concomitant diminution of crystallite particle size.

Although the specific activity exhibits a consistent poisoning coefficient, four other characteristics of the reaction exhibit dependencies on lanthanum concentration: the reaction order on carbon monoxide, the apparent energy of

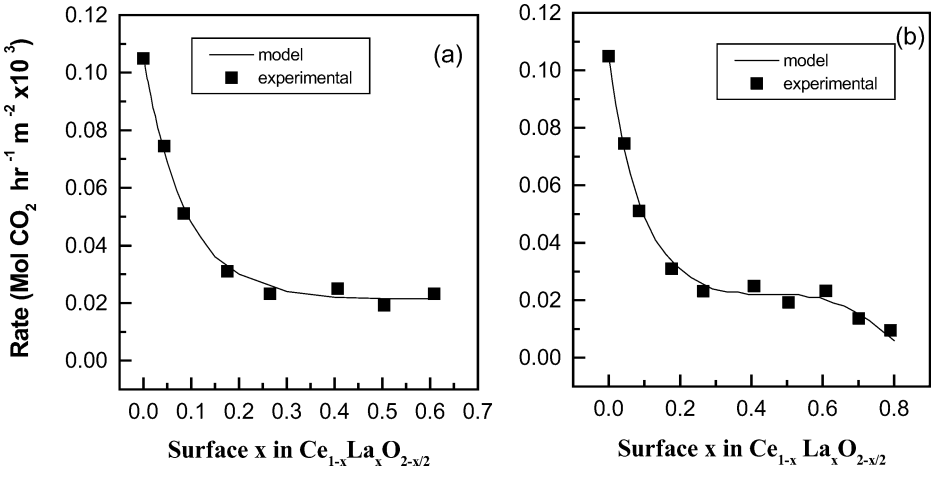

Fig. 9. Specific activity as a function of x_s: experimental points with lines modelled on (a) poisoning by lanthanum and (b) size of active ensembles of cerium.

activation, the pre-exponential factor, and the retardation coefficient of carbon dioxide. On the reaction orders, at the partial pressures of carbon monoxide adopted for the standard tests, the order over ceria is about one whereas over the lanthana-containing catalysts it is negative. The kinetic schemes suppose a kinetically limiting transfer of an adsorbed oxygen species to adsorbed carbon monoxide, monomeric on ceria and dimeric on lanthanum-containing catalysts. The auto-retarding effect of carbon monoxide over lanthanum-containing catalysts is taken as a requirement for a site adjacent to the active ensemble free to adsorb the product carbon dioxide. On the energy term and the pre-exponential factor, these exhibit volcano-style responses to the concentration of surface lanthanum ionic fraction with peaks within the range of ionic fractions 0.1–0.2, most probably at about 0.13. On the retardation by carbon dioxide, it is strong over ceria but weak over lanthana.

Regrettably, the kinetic studies were not sufficiently intensive to enable the form of the change to be monitored with respect to oxide composition. However, the kinetic model over the mixed oxide catalyst examined suitably combines those over the pure oxides. We shall assume there to be an oxide composition-dependent shift from one to the other. We shall further assume that the shapes of the energy of activation and pre-exponential factor as functions of surface lanthanum, x_s, that the range of ionic fractions 0.1–0.2 exhibit a watershed for the change of mechanism; i.e., the ceria-style mechanism operates up to this range but is gradually replaced by the lanthana-style mechanism beyond. We have already noted that the kinetics over $Ce_{0.95}La_{0.05}O_{1.875}$ where x_s is 0.18 corresponds to about 85% of the ceria-style process. Additionally, Fig. 9b suggests that up to x_s of about 0.1–0.2, the apparent size of active cerium ensemble decreases linearly with increasing x_s. Cerium may activate adsorbed monomeric carbon monoxide whereas the lanthanum-containing catalysts may activate an adsorbed dimeric form of carbon monoxide. Bailes et al. [23] report CO coupling on basic oxides such as lanthana to form the ketenide anion, $C_2O_3^{2-}$. We have already shown how, in the present series of catalysts, an increasing level of lanthana raises the basicity [25].

Fluorite-structured oxides doped with low valence ions are amongst the best oxygen-conducting solids. An important common characteristic is the appearance of a marked maximum in the plot of electrical conductivity versus dopant concentration attributed to, at low dopant levels, to the increasing concentration of isolated oxygen vacancies and, at higher levels, to their clustering [26,27]. In the case of lanthana-doped ceria, Takahashi [13] found the temperature-dependent peak conductivity to occur at a lanthanum ionic fraction of 0.11 at 400 °C and at 0.21 at 1200 °C. Extrapolation to 310 °C, the temperature at which the present comparative activity studies were made, places the maximum conductivity at 0.1. Although Takahashi's data refer to conductivity of bulk materials, we shall assume that it is equally applicable to the surface and accordingly propose that maximum surface conductivity would be found at a surface ionic fraction of lanthanum close to that exhibiting peaks in the energy of activation and pre-exponential factor of the present catalytic reaction. Thus the peaks may be associated with a maximum in the concentration of isolated anionic vacancies. Theoretical treatments have already proposed that intrinsic oxygen vacancies play a pivotal role in the catalytic oxidation of carbon monoxide [9–11].

Below the peak, the vacancy population and the energy of activation of electron transfer from adsorbed carbon monoxide increases with lanthanum, whereas above the peak, vacancy clustering ameliorates this trend. Additionally, it may be noted that the modified exponent of the Andersen model (Eq. (11)) included first- and second-order terms in x_s, surface populations of lanthanum and/or oxygen vacancies; these terms may correspond to isolated and clustered defects, respectively.

At temperatures close to the threshold for activity, ceria catalysts doped with the lower valent ions gadolinia and preseodymia are also poisoned relative to that over pure ceria, whereas that doped with the higher valent niobia suffered no such poisoning. Since niobia introduces no extrinsic oxygen ion vacancies, the absence of retardation is consistent with the concepts developed here.

Of ceria-catalysed oxidations, the present retarding effect of lanthanum on the oxidation of carbon monoxide contrasts strongly with its promotional influence on the conversion of methane [25]. The former is attributed to the impedance of electron transfer from an ensemble of cerium atoms; the latter is related to synergism between ceria as an oxidant and lanthana as a base.

References

[1] G. Rienaker, Z. Anorg. Allg. Chem. 258 (1949) 280.
[2] G. Rienaker, M. Birckenstaedt, Z. Anorg. Allg. Chem. 262 (1950) 81.
[3] G. Rienaker, Y. Wu, Z. Anorg. Allg. Chem. 315 (1962) 121.
[4] M. Breysse, B.C. Guenin, B. Clauddel, H. Latrelle, J. Veron, J. Catal. 27 (1972) 275.
[5] M. Breysse, B.C. Guenin, B. Clauddel, J. Veron, J. Catal. 28 (1973) 54.
[6] S.H. Oh, C.C. Eickel, J. Catal. 112 (1988) 543.
[7] T. Jin, G.J. Okuhara, G.J. Mains, J.M. White, J. Phys. Chem. 91 (1987) 3310.
[8] F. Serre, E. Garin, G. Belot, G. Maire, J. Catal. 141 (1993) 9.
[9] T.X.T. Sayle, S.C. Parker, C.R.A. Catlow, J. Chem. Soc. Chem. Commun. (1992) 977.
[10] M.G. Sanchez, J.L. Gasquez, J. Catal. 104 (1987) 120.
[11] T.X.T. Sayle, S.C. Parker, C.R.A. Catlow, Surf. Sci. 316 (1994) 329.
[12] A. Trovarelli, Catal. Rev. Sci. Eng. 38 (1996) 439.
[13] T. Takahashi, in: J. Hladik (Ed.), Physics of Electrolytes, in: Thermodynamics and Electrode Processes in Solid State Electrolytes, Vol. 2, Academic Press, London, 1972.
[14] P.G. Harrison, D.A. Creaser, B.A. Wolfindale, K.C. Waugh, M.A. Morris, W.C. Mackrodt, in: T.J. Dines, C.H. Rochester, J. Thomson (Eds.), Catalysis and Surface Characterisation, in: Royal Society of Chemistry Special Publications, Vol. 114, Royal Society of Chemistry, Cambridge, 1992.
[15] M. Cotter, S. Campbell, C.C. Cao, R.G. Ehgell, W.C. Mackrodt, Surf. Sci. 208 (1989) 267.
[16] W. Liu, M. Flytzani-Stephanopoulos, J. Catal. 153 (1995) 304.

[17] M. Pijolat, M. Prin, M. Soustell, Solid Sate Ionics 63–65 (1993) 789.
[18] F. Zamar, A. Trovarelli, C. de Leitenburg, G. Dolcetti, J. Chem. Soc. Chem. Commun. (1995) 965.
[19] L. Kundakovic, M. Flytzani-Stephanopoulos, J. Catal. 179 (1998) 203.
[20] M.F. Wilkes, P. Hayden, A.K. Bhattacharya, Appl. Surf. Sci. (in press). Refer to the accompanying paper, "Surface segregation of lanthanum and cerium ions in a ceria–lanthana solid solutions."
[21] M. Breysse, M. Guenin, B. Claudel, H. Latreille, J. Véron, J. Catal. 27 (1972) 275.
[22] C. Li, Y. Sakata, T. Arai, K. Domen, K. Maruya, T. Onishi, J. Chem. Soc. Faraday Trans. 1 85 (1989) 929.
[23] M. Bailes, S. Bordiga, F.S. Stone, A. Zecchina, J. Chem. Soc. Faraday Trans. 92 (23) (1996) 4675.
[24] N.T. Andersen, F. Topsoe, I. Alstrup, J.R. Rostrup-Nielsen, J. Catal. 104 (1987) 454.
[25] M.F. Wilkes, P. Hayden, A.K. Bhattacharya, J. Catal. (Part in press).
[26] H. Schmalzried, Z. Phys. Chem. (NF) 105 (1979) 47.
[27] C.R.A. Catlow, Solid State Ionics 12 (1984) 67.